Hindawi Publishing Corporation
Advances in Materials Science and Engineering
Volume 2012, Article ID 409379, 8 pages
doi:10.1155/2012/409379

Research Article

Preparation and Photocatalytic Activity of Magnetic $Fe_3O_4/SiO_2/TiO_2$ Composites

Rijing Wang,[1,2] Xiaohong Wang,[1,2] Xiaoguang Xi,[1,2] Ruanbing Hu,[1,2] and Guohua Jiang[1,2]

[1] *Department of Materials Engineering, College of Materials and Textile, Zhejiang Sci-Tech University, Hangzhou 310018, China*
[2] *Key Laboratory of Advanced Textile Materials and Manufacturing Technology (ATMT) of Ministry of Education, Zhejiang Sci-Tech University, Hangzhou 310018, China*

Correspondence should be addressed to Guohua Jiang, polymer_jiang@hotmail.com

Received 29 October 2011; Accepted 8 December 2011

Academic Editor: Qiang Yang

Copyright © 2012 Rijing Wang et al. This is an open access article distributed under the Creative Commons Attribution License, which permits unrestricted use, distribution, and reproduction in any medium, provided the original work is properly cited.

A simple sol-gel method was used to prepare magnetic $Fe_3O_4/SiO_2/TiO_2$ composites with core-shell structure. Fourier transform infrared spectroscopy (FT-IR), X-ray diffraction (XRD), field emission scanning electron microscopy (FE-SEM), and transmission electron microscopy (TEM) have been applied to investigate the structure and morphology of the resultant composites. The obtained composites showed excellent magnetism and higher photodegradation ability than pure TiO_2. The photocatalytic mechanism was also discussed. The magnetic composites should be extended to various potential applications, such as photodegradation, catalysis, separation, and purification processes.

1. Introduction

Currently, there has been great interest in the preparation of core-shell micro- and nanoparticles for their widespread potential applications in catalysis, chromatography separation, drug delivery, chemical reactors, and protection of environmentally sensitive materials [1–4]. Heterogeneous photocatalysis using semiconducting oxide catalysts is an effective way to purify wastewater or gas. TiO_2-based semiconductors have attracted considerable attention due to their high efficiency, good stability, availability, and nontoxicity [5–9]. In recent years, in order to enhance the photocatalytic activity, great efforts have been made to prepare ideal structure of TiO_2-based semiconductors [10–12].

Magnetic separation provides a very convenient approach for removing and recycling magnetic composites by applying an added magnetic field. The incorporation of Fe_3O_4 magnetic particles into TiO_2 matrix may block the aggregation of nanoparticles during renewal and can increase the durability of the catalysts [13, 14]. Moreover, such catalysts have a high surface area and well-defined pore size, which enhance their photocatalytic activity [15]. However, magnetic nanoparticles would inescapably encounter an hindrance when applied in practice due to the fact that a photocatalytic reaction is conducted in a suspension. It is not allowed to use magneton to agitate the mixed solutions. Therefore, in the experiment, Ar gas is purged so as to make the magnetic particles suspend in the methylene blue (MB) solution.

Many efforts have been made in the development of the design and preparation of magnetic core-shell microspheres. Ye et al. and Yu et al. reported the magnetic material/SiO_2 /TiO_2 composites with core-shell-shell structure [16, 17]. Their methods involve superparamagnetic Fe_3O_4 and γ-Fe_2O_3 with an inner layer of SiO_2 and outer layer of TiO_2 [18, 19]. Their resultant samples exhibit superior photodegradation ability and can be easily recycled by applying an external magnetic field. Zhou et al. reported the preparation of core-shell structure of Fe_3O_4/SiO_2 nanospheres via a modified inverse emulsion process [20]. Many methods have been applied to prepare composites with core-shell structure. However, it remains a great challenge to explore a feasible, easily controllable, and repeatable method for the preparation of core-shell nanostructure composites.

Nanosize TiO_2 exhibits superior photocatalytic activity compared to the common TiO_2 because of its rough surface and larger pore volumes. Herein, we directly use the Fe_3O_4 nanoparticles (a mean diameter of approximately 20 nm) as

the core of the composites, then a inner layer of SiO_2 and outer layer of TiO_2 were coated via a simple sol-gel process and a rapid combustion process. Silica coating is a necessary step to prepare core-shell structure because the hydrophobic Fe_3O_4 nanoparticles cannot be easily encapsulated in a TiO_2 shell [21]. Moreover, SiO_2 can be selectively etched onto the hollow magnetic/TiO_2 microspheres, allowing enough spaces for uploading some materials that can absorb polluted gas or wastewater. In the photocatalytic experiment, the pH of solution effect on the photocatalytic activity of catalyst was investigated and peroxide solution (30%) was added to enhance the catalyst activity through promoting the formation of hydroxyl radical and the reduced rate of interfacial electron transfer. This may open up new possibilities to synthesize core-shell structure for other composites and extend their applications.

2. Experimental Section

2.1. Materials and Reagents. Nanoiron (II, III) oxide (spherical, diameter 20 nm, 99.5%) was purchased from Shanghai Chemical Co., Ltd., China. Ammonia solution and isopropyl alcohol were obtained from Hangzhou High-Crystal Fine Chemical Co., Ltd., China. Tetraethoxysilane (TEOS) and tetrabutyltitanate (TBOT) were purchased from Tianjin Kermel Chemical Reagent Co., Ltd., China. Anhydrous ethanol was obtained from Hangzhou Changzheng Chemical Reagent Co., Ltd., China. Pure TiO_2 was purchased from Degussa Co. Ltd. All reagents were used without further purification. Deionized water was used in all experiments.

2.2. Preparation of Fe_3O_4/SiO_2 Nanospheres. The Fe_3O_4 nanoparticles (0.25 g) were ultrasonicated for 1 h to make them uniformly disperse in anhydrous ethanol (40 mL). Concentrated ammonium hydroxide (4.5 mL) was diluted to the above solution, and TEOS (0.8 mL) was quickly added under vigorous stirring. The solution was left to stir for 12 h. The product was collected by centrifugation and washed with anhydrous ethanol three times.

2.3. Preparation of Pomegranate-Like $Fe_3O_4/SiO_2/TiO_2$ Composite Microspheres. The resultant Fe_3O_4/SiO_2 nanocomposites were redispersed in anhydrous ethanol (40 mL). Subsequently, a proper amount of TBOT (1 mL) dissolved in isopropyl alcohol (8 mL) was introduced to the system dropwise, followed by heating the solution at about 70°C. The whole process was under vigorous stirring. After 12 h, the red brown precipitates were washed with deionized water and ethanol five times and dried in a vacuum oven at 60°C for 8 h. Finally, the products were calcined in air at 500°C for 2 h.

2.4. Characterization. X-ray diffraction (XRD) patterns were analyzed by X-ray diffractometer using Cu Kα radiation source at 35 kV, with a scan rate of 0.1° $2\theta\,s^{-1}$ in the 2θ range of 10–80°. The morphology and microstructure of products were characterized by ULTRA-55 field-emission scanning electron microscopy (FE-SEM) and JSM-2100 transmission electron microscopy (TEM) equipped with an energy dispersive X-ray spectrum (EDS, Inca Energy-200) at an accelerating voltage of 200 kV. Fourier transform infrared (FT-IR) spectra were recorded on a Nicolet 5700 spectrophotometer using KBr pellets for samples.

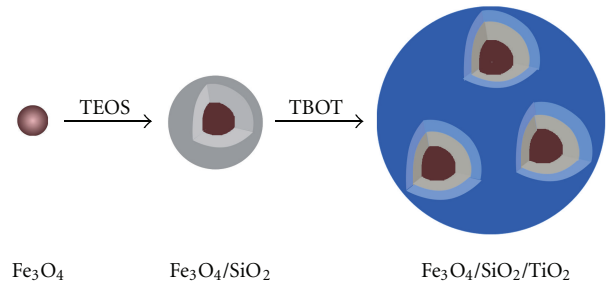

Scheme 1: The schematic process for preparing $Fe_3O_4/SiO_2/TiO_2$ composites.

2.5. Photocatalytic Activity Evaluation. The photocatalytic activity of $Fe_3O_4/SiO_2/TiO_2$ composites was investigated by the photodegradation of MB aqueous solution at ambient temperature. The photodegradation experiments were carried out in a closed box, of which UV radiation source is 100 W high-pressure mercury lamp, its wavelength range is 290−450 nm, and the peak intensity is 365 nm (Model OCRS-I, Kaifeng Hxsei Science Instrument Factory, China). No pure oxygen was supplied because it has enough oxygen for oxidation photodegradation under continuously stirring in atmosphere in previous experiment [22, 23]. The initial MB concentration (C_0) was 30 mg/L, the photocatalyst concentration was 0.5 g/L, and the pH of the solution was adjusted to 2, 7, and 10 with hydrochloric acid and sodium hydroxide solution. Before switching on the mercury, we passed Ar gas into the mixture solution of MB and photocatalyst in a dark condition for 30 min to achieve adsorption balance. The concentration of MB (C_t) was analyzed through JASCO V-570 UV/Vis/NiR spectrophotometer at $\lambda_{max} = 664$ nm. The concentration of MB (C_t) can be obtained by the following formula (where k is a constant):

$$A = k \times C. \tag{1}$$

Acetic acid (5 vol%, 5 mL) was also used to be photodegraded with $Fe_3O_4/SiO_2/TiO_2$ composites (20 mg) and pure TiO_2 using the aforementioned method. The amount of evolved CO_2 was determined by a gas chromatograph (GC, Agilent 6890).

3. Results and Discussion

The formation of $Fe_3O_4/SiO_2/TiO_2$ composites can be divided into two steps (Scheme 1). The first step is the hydrolyzation of TEOS on the Fe_3O_4 nanoparticles by the classical Stöber method; the silica layer can be easily coated on the surface of Fe_3O_4 nanoparticles. Some Fe_3O_4/SiO_2 nanoparticles would be aggregated, and the hydrolyzation of TBOT on the Fe_3O_4/SiO_2 composites resulted in the formation of pomegranate-like structure.

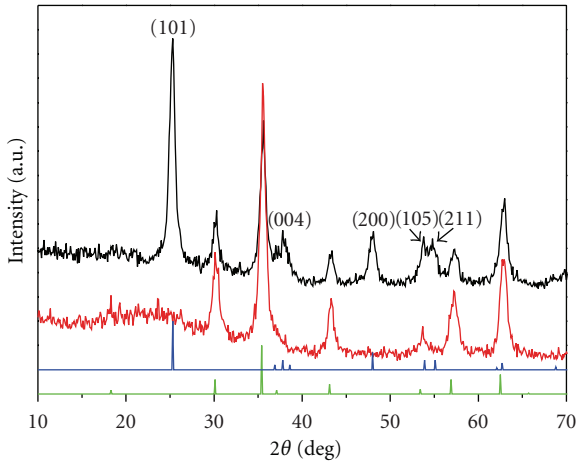

(A) Fe_3O_4/SiO_2 (C) JCPDS 19-0629
(B) $Fe_3O_4/SiO_2/TiO_2$ (D) JCPDS 21-1272

Figure 1: XRD pattern of Fe_3O_4/SiO_2 (A) and $Fe_3O_4/SiO_2/TiO_2$ composites (B).

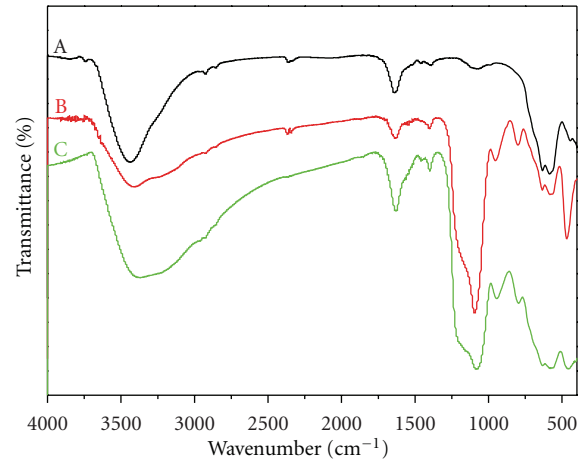

(A) Fe_3O_4
(B) Fe_3O_4/SiO_2
(C) $Fe_3O_4/SiO_2/TiO_2$

Figure 2: FT-IR spectra of Fe_3O_4 (A), Fe_3O_4/SiO_2 (B), and $Fe_3O_4/SiO_2/TiO_2$ composites (C).

The Fe_3O_4/SiO_2 and $Fe_3O_4/SiO_2/TiO_2$ composites were characterized by XRD. As shown in Figure 1(A), all peaks can be indexed as the magnetite phase of Fe_3O_4 (JCPDS 19-0629). No characteristic peaks of SiO_2 were detected, indicating that the SiO_2 was amorphous. In contrast to Figure 1(A), the successful TiO_2 coating was confirmed by the presence of the new peaks (Figure 1(B)). The reduction of Fe_3O_4 peaks also confirmed the successful TiO_2 coating. The as-prepared samples displayed good crystallinity; and the TiO_2 peaks can be ascribed to the (101), (004), (200), (105), and (211) planes of anatase phase (JCPDS 21-1272). According to the Scherrer equation,

$$D = \frac{0.89\lambda}{(\gamma \cos\theta)}, \quad (2)$$

where D is the average crystallite size, the factor 0.89 is characteristic of spherical objects, λ is the X-ray wavelength, γ and θ are the full width at half-maximum and diffraction angle of an observed peak, respectively. The primary crystallite size calculated from the (101) peak of the XRD pattern was about 12.64 nm.

FT-IR was used to characterize the composition and structure of the Fe_3O_4, Fe_3O_4/SiO_2, and $Fe_3O_4/SiO_2/TiO_2$ composites. As shown in Figure 2, the $Fe_3O_4/SiO_2/TiO_2$ composites possess more signals than Fe_3O_4. It has been reported that the signal at the wave number around 800 cm^{-1} corresponds to the symmetric vibration of Si–O–Si, 1080 cm^{-1} for asymmetric stretching vibration of Si–O–Si, and 940–960 cm^{-1} for Si–O–Ti vibration and 500–900 cm^{-1} originates from Ti–O–Ti [24, 25]. Silica presence as an amorphous phase was confirmed by combining the results of FT-IR and XRD. The presence of water is evidenced by the appearance of the bending mode at 1630 cm^{-1} and the stretching mode at 3370 cm^{-1}. This surface hydroxylation is advantageous for the photocatalytic activity of $Fe_3O_4/SiO_2/TiO_2$ microspheres because it provides higher capacity for oxygen adsorption [26].

The morphology and structure of the as-prepared samples were investigated by field emission scanning electron microscopy (FE-SEM). Figure 3(a) shows that the Fe_3O_4 nanoparticles are of a diameter of 20 ± 2 nm. They prefer to gather together due to their small size and magnetic. The grape-like Fe_3O_4/SiO_2 nanospheres with a diameter of 25 ± 2 nm are shown in Figure 3(b). This indicated that SiO_2 was successfully coated on the Fe_3O_4 nanoparticles. Figures 3(c) and 3(d) present typical FE-SEM images of as-prepared $Fe_3O_4/SiO_2/TiO_2$ composites. These images indicate that the surfaces of $Fe_3O_4/SiO_2/TiO_2$ microspheres are rough and porous, which favor enhancing the photocatalytic activity [27]. A large number of Fe_3O_4/SiO_2 nanospheres are encapsulated in the core of TiO_2 shell, forming the pomegranate-like structure, which can make the dyes better contact with the catalysts so as to achieve the purpose of degradation [28].

The morphology and structure of the resultant samples were further investigated by transmission electron microscopy (TEM) (Figure 4). As expected, the Fe_3O_4/SiO_2 nanospheres were composed of aggregated spherical particles with sizes around 25 nm. Moreover, a large number of nanoparticles are encapsulated in the SiO_2 layer (Figure 4(a)). In contrast to the morphology of Fe_3O_4/SiO_2 nanoparticles, Figure 4(b) clearly displays that TiO_2 was successfully coated on Fe_3O_4/SiO_2 nanoparticles. The EDS pattern (Figure 5) taken from this area shows the presence of only Fe, Si, Ti, and O elements.

Magnetic separation provides a very convenient approach for removing and recycling magnetic catalysts. The magnetism of $Fe_3O_4/SiO_2/TiO_2$ composites was confirmed by Figure 6, and the $Fe_3O_4/SiO_2/TiO_2$ composites were tested in water by placing a magnet near the glass bottle. The red brown particles can be attracted toward the magnet

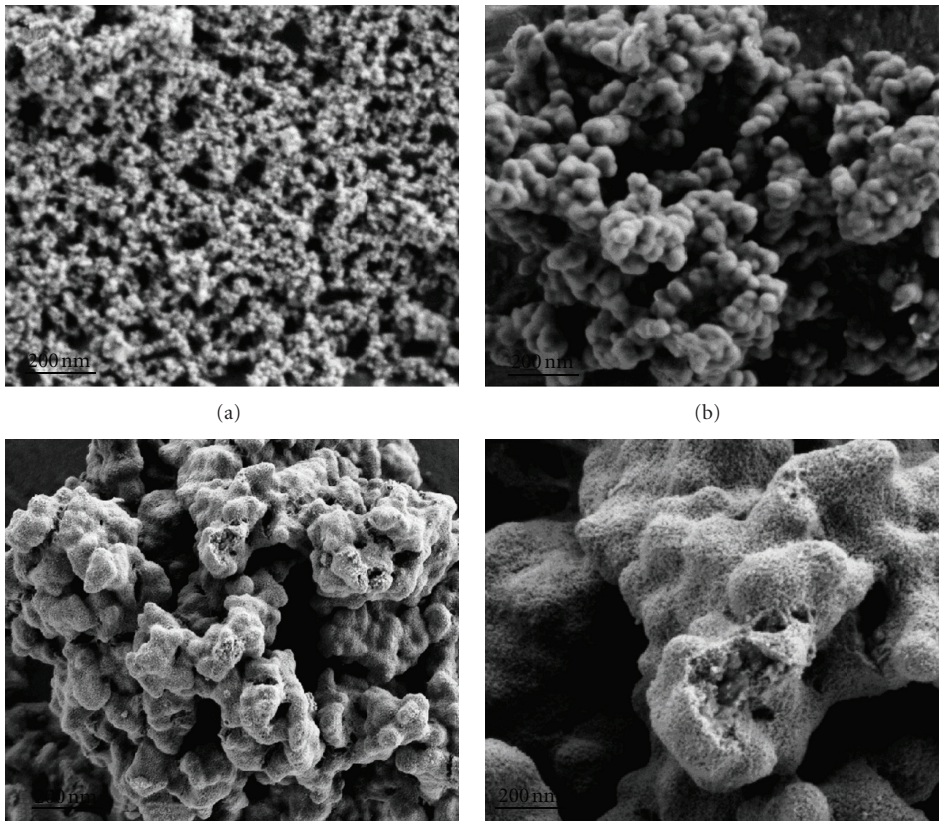

Figure 3: FE-SEM images of Fe_3O_4 (a) and Fe_3O_4/SiO_2 (b) $Fe_3O_4/SiO_2/TiO_2$ composite microspheres (c, d).

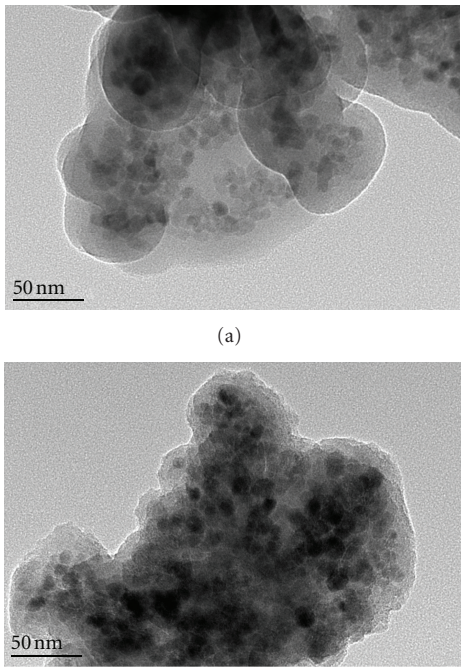

Figure 4: TEM images of Fe_3O_4/SiO_2 (a) and $Fe_3O_4/SiO_2/TiO_2$ composite microspheres (b).

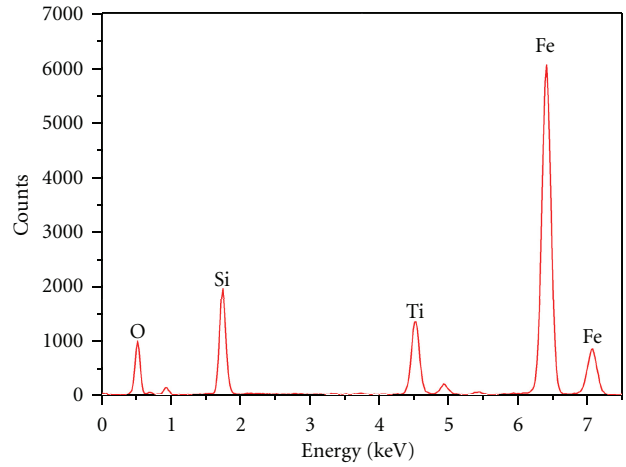

Figure 5: EDS pattern of $Fe_3O_4/SiO_2/TiO_2$ composites calcined at 500°C for 2 h.

with time increasing, and the $Fe_3O_4/SiO_2/TiO_2$ almost totally attracted after 5 min, leaving a clear solution. So the as-prepared samples can be easily recycled after the achievement of photocatalytic process.

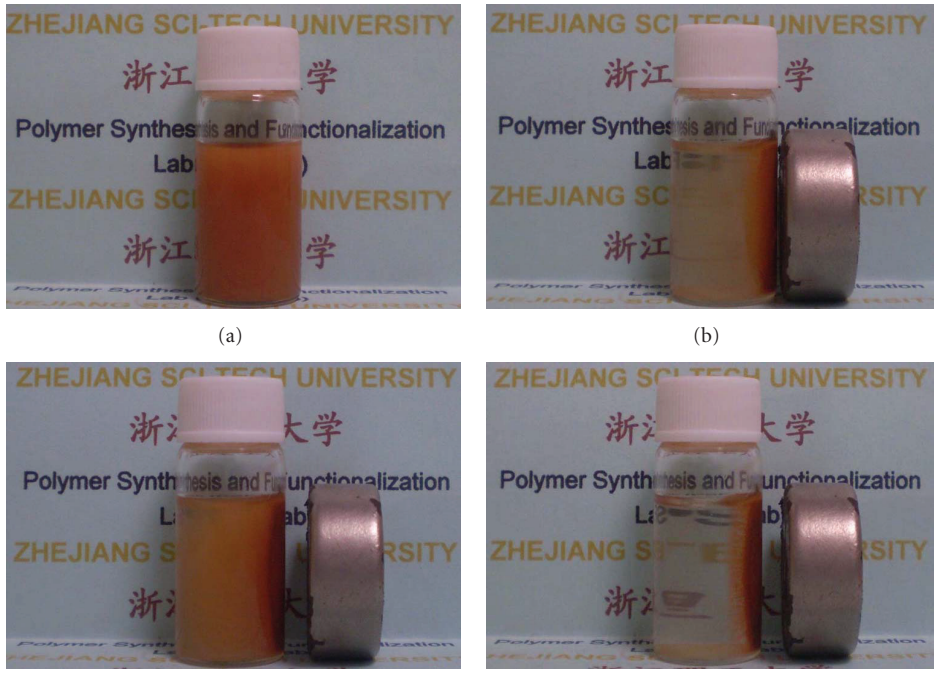

Figure 6: Digital illumination photographs of $Fe_3O_4/SiO_2/TiO_2$ composites separated from solution by applying an added magnet ((a) 0 min, (b) 1 min, (c) 2 min, and (d) 5 min).

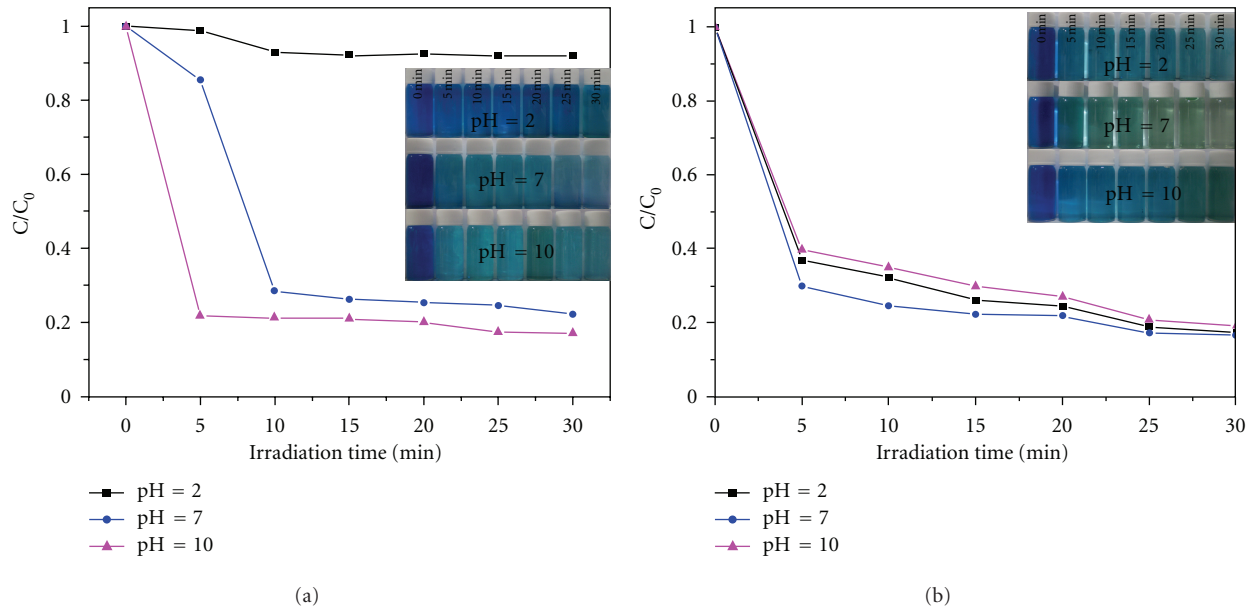

Figure 7: Photodegradation efficiency of $Fe_3O_4/SiO_2/TiO_2$ composite microspheres and digital illumination photographs at pH 2, 7, and 10 ((a) with 1 mL H_2O; (b) with 1 mL H_2O_2).

Figure 7 depicts the photocatalytic activity of $Fe_3O_4/SiO_2/TiO_2$ composites and shows the digital illumination photographs of MB aqueous solution under UV light irradiation at different pH values with H_2O_2 or without. In the experiment, we used the deionized water as the blank, comparing with H_2O_2 to ensure only a variable. Figure 7(a) shows that the rate of photodegradation of MB was higher at the neutral and alkaline environment. 78% photodegradation of MB solution (pH = 10) was observed after 5 min under UV irradiation. However, in the acidic condition, only 8.5% of MB has been photodegraded after 30 min. As shown in the digital illumination photographs of MB aqueous solution under UV light irradiation at different pH values. The color of MB solution fades gradually with irradiation time at

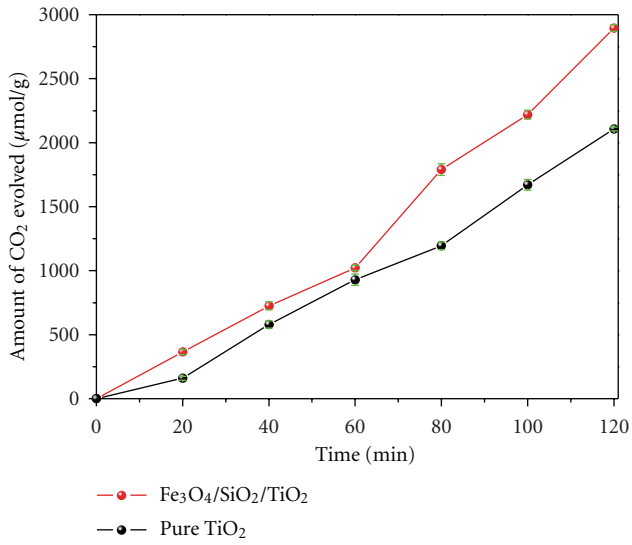

Figure 8: Relationship between the amount of CO_2 evolved and irradiation time for photocatalytic degradation of acetic acid aqueous solution.

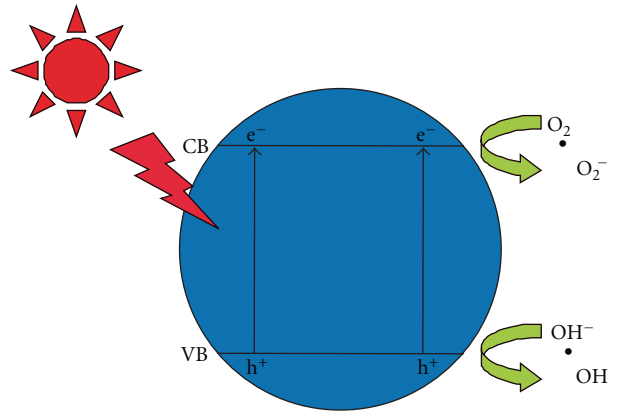

Scheme 2: The scheme of photocatalytic mechanism of $Fe_3O_4/SiO_2/TiO_2$ composite microspheres.

pH = 7 and 10, but with no distinct change of the color at pH = 2. This is because the pH influenced the adsorption property of organic compounds and their dissociating state in solution. The surface charge properties of TiO_2 were also changed with the changes in pH value due to amphoteric behavior of semiconducting TiO_2 [29]. It is interesting to see from Figure 7(b) that photodegradation efficiency of MB at different pH values with H_2O_2 can reach 60% after 5 min under UV irradiation. H_2O_2 enhanced the photodegradation ability attributed to its electron acceptor behavior, which reacted with conduction band electrons to generate hydroxyl radicals. The point of zero charge (pzc) for titanium dioxide is at pH 6.5. The TiO_2 surface is positively charged in acidic solution and negatively charged in basic solution [30]. Since MB is a cationic dye, it is conceivable that, at higher pH value, its adsorption is favored on a negatively charged surface.

In order to demonstrate the photocatalytic activity of $Fe_3O_4/SiO_2/TiO_2$ composites, acetic acid was selected as a model organic acid. As shown in Figure 8, the amount of CO_2 evolution increases with irradiation time for pure TiO_2 and $Fe_3O_4/SiO_2/TiO_2$. However, in case of $Fe_3O_4/SiO_2/TiO_2$, the yield rate of CO_2 reaches about $1448.05 \pm 6.25\,\mu\text{mol}\,\text{h}^{-1}\,\text{g}^{-1}$, which is higher than pure TiO_2 ($1053.12 \pm 7.23\,\mu\text{mol}\,\text{h}^{-1}\,\text{g}^{-1}$) for 2 h. The higher CO_2 evolution rate for $Fe_3O_4/SiO_2/TiO_2$ sample may be attributed to rough and porous surface of $Fe_3O_4/SiO_2/TiO_2$ composites, which enhances the photocatalytic activity by facilitating the access to the reactive TiO_2.

The schematic illustration of the charge transfer by $Fe_3O_4/SiO_2/TiO_2$ composites is summarized in Scheme 2. Photoexcitation of the $Fe_3O_4/SiO_2/TiO_2$ composites likely results in charge separation to form electrons and holes (3) [31]. Photo-generated electrons can directly react with the absorbed O_2 molecules to form $\cdot O_2^-$ active species (4). Photogenerated electrons also capture H_2O_2 molecules to produce $\cdot$OH and OH^- (5). The resultant $\cdot O_2^-$ can react with H_2O_2 to form $\cdot$OH and OH^- (6). The obtained OH^- can react with photogenerated holes to generate the hydroxyl free radical $\cdot$OH (7) [32]. Both $\cdot O_2^-$ and $\cdot$OH can photodegrade the MB solution:

$$TiO_2 + h\nu \longrightarrow TiO_2 + h^+ + e^- \quad (3)$$

$$O_2 + e^- \longrightarrow O_2^- \quad (4)$$

$$H_2O_2 + e^- \longrightarrow \bullet OH + OH^- \quad (5)$$

$$H_2O_2 + O_2^- \longrightarrow \bullet OH + OH^- \quad (6)$$

$$OH^- + h^+ \longrightarrow \bullet OH. \quad (7)$$

H_2O_2 enhanced photodegradation ability attributed to its electron acceptor behavior, which reacted with conduction band electrons to generate hydroxyl radicals.

4. Conclusion

In summary, the magnetic $Fe_3O_4/SiO_2/TiO_2$ composites have been prepared by a simple sol-gel method. The morphology and structure of the resultant samples were characterized by FT-IR, XRD, FE-SEM, and TEM. The $Fe_3O_4/SiO_2/TiO_2$ composites show excellent magnetism and higher photocatalytic activity than pure TiO_2 attributed to rough and porous surface of $Fe_3O_4/SiO_2/TiO_2$ composites, which enhances the photocatalytic activity by facilitating the access to the reactive TiO_2. The photocatalytic mechanism was also discussed. The magnetic $Fe_3O_4/SiO_2/TiO_2$ composites should be extended to various potential applications, such as photocatalysis, separation, and purification processes.

Acknowledgments

This work was financially supported by the Qianjiang Talents Project of Zhejiang Province (2010R10023), the Scientific Research Foundation for the Returned Overseas Chinese Scholars, the State Education Ministry (1001603-C), the Natural Science Foundation of Zhejiang Province

(Y4100045, Y4080392, R210101054), Foundation of Zhejiang Province New Textile Research and Development Emphasised Laboratory (2009FZD001), the Key Bidding Project of Zhejiang Provincial Key Lab of Fiber Materials and Manufacturing Technology, Zhejiang Sci-Tech University (S2010002), and the Program for Changjiang Scholars and Innovative Research Team in University (PCSIRT: 0654).

References

[1] F. Caruso, R. A. Caruso, and H. Möhwald, "Nanoengineering of inorganic and hybrid hollow spheres by colloidal templating," *Science*, vol. 282, no. 5391, pp. 1111–1114, 1998.

[2] R. A. Caruso, A. Susha, and F. Caruso, "Multilayered titania, silica, and Laponite nanoparticle coatings on polystyrene colloidal templates and resulting inorganic hollow spheres," *Chemistry of Materials*, vol. 13, no. 2, pp. 400–409, 2001.

[3] F. Caruso, X. Shi, R. A. Caruso, and A. Susha, "Hollow titania spheres from layered precursor deposition on sacrificial colloidal core particles," *Advanced Materials*, vol. 13, no. 10, pp. 740–744, 2001.

[4] G. Li, Q. Shi, S. J. Yuan, K. G. Neoh, E. T. Kang, and X. Yang, "Alternating silica/polymer multilayer hybrid microspheres templates for double-shelled polymer and inorganic hollow microstructures," *Chemistry of Materials*, vol. 22, no. 4, pp. 1309–1317, 2010.

[5] J. M. Herrmann, "Heterogeneous photocatalysis: fundamentals and applications to the removal of various types of aqueous pollutants," *Catalysis Today*, vol. 53, no. 1, pp. 115–129, 1999.

[6] Z. Xu and J. Yu, "Visible-light-induced photoelectrochemical behaviors of Fe-modified TiO_2 nanotube arrays," *Nanoscale*, vol. 3, no. 8, pp. 3138–3144, 2011.

[7] H. Li, Z. Bian, J. Zhu, Y. Huo, H. Li, and Y. Lu, "Mesoporous Au/TiO_2 nanocomposites with enhanced photocatalytic activity," *Journal of the American Chemical Society*, vol. 129, no. 15, pp. 4538–4539, 2007.

[8] H. Q. Wang, Z. B. Wu, and Y. Liu, "A simple two-step template approach for preparing carbon-doped mesoporous TiO_2 hollow microspheres," *Journal of Physical Chemistry C*, vol. 113, no. 30, pp. 13317–13324, 2009.

[9] X. Chen and S. S. Mao, "Titanium dioxide nanomaterials: synthesis, properties, modifications and applications," *Chemical Reviews*, vol. 107, no. 7, pp. 2891–2959, 2007.

[10] J. C. Lee, T. G. Kim, W. Lee, S. H. Han, and Y. M. Sung, "Growth of CdS nanorod-coated TiO_2 nanowires on conductive glass for photovoltaic applications," *Crystal Growth and Design*, vol. 9, no. 10, pp. 4519–4523, 2009.

[11] R. A. Lucky, R. Sui, J. M. H. Lo, and P. A. Charpentier, "Effect of solvent on the crystal growth of one-dimensional $ZrO_2 \cdot TiO_2$ nanostructures," *Crystal Growth and Design*, vol. 10, no. 4, pp. 1598–1604, 2010.

[12] S. Xuan, W. Jiang, X. Gong, Y. Hu, and Z. Chen, "Magnetically separable Fe_3O_4/TiO_2 hollow spheres: fabrication and photocatalytic activity," *Journal of Physical Chemistry C*, vol. 113, no. 2, pp. 553–558, 2009.

[13] W. Cheng, K. Tang, Y. Qi, J. Sheng, and Z. Liu, "One-step synthesis of superparamagnetic monodisperse porous Fe_3O_4 hollow and core-shell spheres," *Journal of Materials Chemistry*, vol. 20, no. 9, pp. 1799–1805, 2010.

[14] Z. Liu, H. Bai, and D. D. Sun, "Facile fabrication of porous chitosan/TiO_2/Fe_3O_4 microspheres with multifunction for water purifications," *New Journal of Chemistry*, vol. 35, no. 1, pp. 137–140, 2011.

[15] M. Shokouhimehr, Y. Piao, J. Kim, Y. Jang, and T. Hyeon, "A magnetically recyclable nanocomposite catalyst for olefin epoxidation," *Angewandte Chemie—International Edition*, vol. 46, no. 37, pp. 7039–7043, 2007.

[16] M. M. Ye, Q. Zhang, Y. X. Hu et al., "Magnetically recoverable core-shell nanocomposites with enhanced photocatalytic activity," *Chemistry—A European Journal*, vol. 16, no. 21, pp. 6243–6250, 2010.

[17] X. Yu, S. Liu, and J. Yu, "Superparamagnetic γ-$Fe_2O_3/SiO_2/TiO_2$ composite microspheres with superior photocatalytic properties," *Applied Catalysis B*, vol. 104, no. 1-2, pp. 12–20, 2011.

[18] W. Stöber, A. Fink, and E. Bohn, "Controlled growth of monodisperse silica spheres in the micron size range," *Journal of Colloid And Interface Science*, vol. 26, no. 1, pp. 62–69, 1968.

[19] J. W. Lee, M. R. Othman, Y. Eom, T. G. Lee, W. S. Kim, and J. Kim, "The effects of sonification and TiO_2 deposition on the micro-characteristics of the thermally treated SiO_2/TiO_2 spherical core-shell particles for photo-catalysis of methyl orange," *Microporous and Mesoporous Materials*, vol. 116, no. 1-3, pp. 561–568, 2008.

[20] J. Zhou, L. Meng, Q. Lu, J. Fu, and X. Huang, "Superparamagnetic submicro-megranates: Fe_3O_4 nanoparticles coated with highly cross-linked organic/inorganic hybrids," *Chemical Communications*, no. 42, pp. 6370–6372, 2009.

[21] C. Hui, C. Shen, J. Tian et al., "Core-shell Fe_3O_4/SiO_2 nanoparticles synthesized with well-dispersed hydrophilic Fe_3O_4 seeds," *Nanoscale*, vol. 3, no. 2, pp. 701–705, 2011.

[22] Y. Chen, K. Wang, and L. Lou, "Photodegradation of dye pollutants on silica gel supported TiO_2 particles under visible light irradiation," *Journal of Photochemistry and Photobiology A*, vol. 163, no. 1-2, pp. 281–287, 2004.

[23] G. Jiang, X. Zheng, Y. Wang, T. Li, and X. Sun, "Photo-degradation of methylene blue by multi-walled carbon nanotubes/TiO_2 composites," *Powder Technology*, vol. 207, no. 1–3, pp. 465–469, 2011.

[24] K. Y. Jung and S. B. Park, "Enhanced photoactivity of silica-embedded titania particles prepared by sol-gel process for the decomposition of trichloroethylene," *Applied Catalysis B*, vol. 25, no. 4, pp. 249–256, 2000.

[25] Z. Ding, G. Q. Lu, and P. F. Greenfield, "Role of the crystallite phase of TiO_2 in heterogeneous photocatalysis for phenol oxidation in water," *Journal of Physical Chemistry B*, vol. 104, no. 19, pp. 4815–4820, 2000.

[26] Z. Liu, X. Quan, H. Fu, X. Li, and K. Yang, "Effect of embedded-silica on microstructure and photocatalytic activity of titania prepared by ultrasound-assisted hydrolysis," *Applied Catalysis B*, vol. 52, no. 1, pp. 33–40, 2004.

[27] J. Yu, X. Yu, B. Huang, X. Zhang, and Y. Dai, "Hydrothermal synthesis and visible-light photocatalytic activity of novel cage-like ferric oxide hollow spheres," *Crystal Growth and Design*, vol. 9, no. 3, pp. 1474–1480, 2009.

[28] J. Yu, L. Zhang, B. Cheng, and Y. Su, "Hydrothermal preparation and photocatalytic activity of hierarchically sponge-like macro-/mesoporous Titania," *Journal of Physical Chemistry C*, vol. 111, no. 28, pp. 10582–10589, 2007.

[29] G. Jiang, R. Wang, H. Jin et al., "Preparation of Cu_2O/TiO_2 composite porous carbon microspheres as efficient visible light-responsive photocatalysts," *Powder Technology*, vol. 212, no. 1, pp. 284–288, 2011.

[30] R. J. Wang, G. H. Jiang, Y. W. Ding et al., "Photocatalytic activity of heterostructures based on TiO_2 and halloysite nanotubes," *ACS Applied Materials and Interfaces*, vol. 3, no. 10, pp. 4154–4158, 2011.

[31] L. Cao, S. Sahu, P. Anilkumar et al., "Carbon nanoparticles as visible-light photocatalysts for efficient CO_2 conversion and beyond," *Journal of the American Chemical Society*, vol. 133, no. 13, pp. 4754–4757, 2011.

[32] Q. Xiang, J. Yu, and P. K. Wong, "Quantitative characterization of hydroxyl radicals produced by various photocatalysts," *Journal of Colloid and Interface Science*, vol. 357, no. 1, pp. 163–167, 2011.

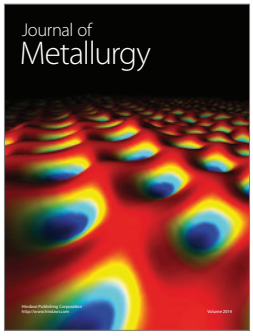

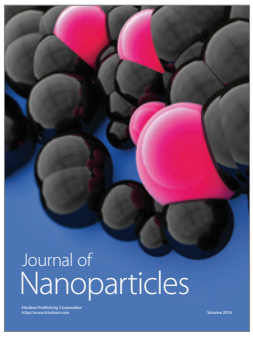

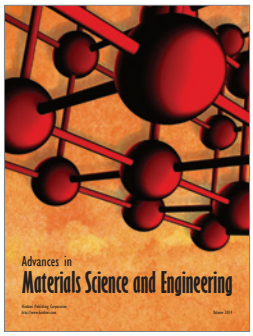

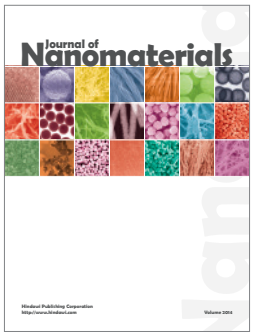

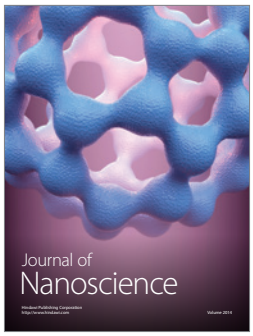

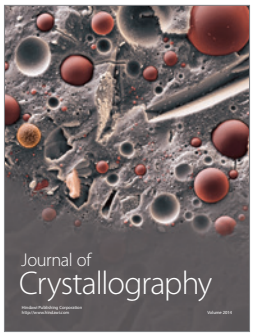

Hindawi

Submit your manuscripts at
http://www.hindawi.com